

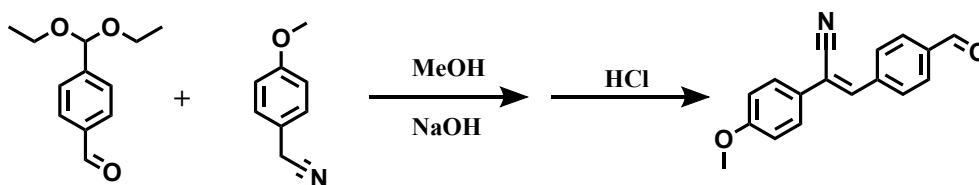
Supporting Information

Multi-Stimuli Responsive Organic Polymorphic Crystals:
Anisotropic Elasticity and Plasticity, Mechanochromism and
Photomechanical Motions

Zhicheng Jiang, Hongtu Zhao, Wenbo Wu, Kui Chen, Hui Yu, Ting Wang, Xin*

*Huang, Na Wang, Lina Zhou and Hongxun Hao**

Molecular Synthesis



Scheme S1 Synthesis of (Z)-3-(4-formylphenyl)-2-(4-methoxyphenyl)acrylonitrile.

Under air atmosphere, (diethoxymethyl)benzaldehyde (416.5 mg, 2 mmol) and (4-methoxyphenyl)acetonitrile (294.3 mg, 2 mmol) were dissolved in 8 mL methanol. Then sodium hydroxide (80 mg, 2 mmol) was added in it and the mixture was stirred for 12 h. The color of mixture was turned to yellow gradually. TLC detection showed that the starting materials were consumed. To the solution, concentrated HCl solution (4 mL) was added and stirred by reflux conditions. The precipitate was formed. The precipitate was filtered and purified by recrystallization in MeOH/water (1:1, V/V). After dryness, (Z)-FMA was collected as yellow solid in yield of 65%.

General Characterization

Molecular structures were confirmed by ^1H NMR spectra on a Bruker 400 MHz spectrometer using the chloroform-d (CDCl_3) solution as the solution. Powder X-ray diffraction (PXRD) was performed on a Rigaku D/MAX 2500 with the parameters of Cu K α radiation are 1.5405 Å, 2-35° and 8°/min. Raman spectra of Form I crystal were recorded respectively using a micro-Raman spectrometer (inVia Reflex, Renishaw) with an excitation wavelength of 785 nm (diode laser) at a spectral resolution of 1 cm^{-1} . Thermal properties were determined by DSC analysis (Model name, Mettler Toledo, Co., Switzerland), with heating and cooling rates of 2°C/min. Fluorescence spectra, quantum yields and lifetimes of solid samples were measured by a photoluminescence spectrometer (Edinburgh Instruments, FLS1000, UK). UV-vis absorption spectra of solid sample were recorded with a spectrophotometer (Hitachi, UV-3010, Japan).

The force-induced mechanical behaviors and photoinduced deformation behaviors were observed by a digital high-speed microscope (Keyence, VHX-5000,

Japan). The microscope images of photoluminescence were taken by Nikon E200. Scanning electron microscopy (SEM) images were captured by Hitachi TM3000.

Theoretical Calculations

The crystal habit of Form II and Form III were simulated by Materials Studio 07. The molecular dipoles of Form III were calculated by Gaussian 09 based on the molecular geometry from single-crystal X-ray analysis at the (time-dependent) DFT B3LYP level, using the B3LYP/6-31G (d, p) model. The optimized geometries of “ σ -dimer ([2+2] cycloadducts)” was calculated by Gaussian 09 based on the B3LYP/6-31G (d, p) model. Energy frameworks was calculated by CrystalExplore 17 software based on the B3LYP/6-31G (d, p) model. Pairwise interaction energies were calculated within a radius of 3.8 Å from the centroids of adjacent molecule.

Nanoindentation tests

The nanoindentation tests were performed on the (001) and (010) planes of Form I by Nanomechanical Test Instrument (Hysitron Inc., TI Premier, USA) with a Berkovich diamond tip indenting the crystals. All the crystals were firmly fixed on the same stage using a cyanoacrylate glue. A peak load, P_{\max} , of 5 mN with a loading/unloading rate of 1 mN/s and hold time of 2 s were used in all cases. The elastic modulus and hardness were calculated by the standard Oliver-Pharr method¹:

$$\frac{1}{E_r} = \frac{(1-\nu^2)}{E} + \frac{(1-\nu_i^2)}{E_i}$$
$$S = \frac{dP}{dh} = \frac{2}{\sqrt{\pi}} E_r \sqrt{A}$$
$$H = \frac{P_{\max}}{A}$$

where E and ν are Young's modulus and Poisson' ratio for the sample, E_i and ν_i are the same parameters for the indenter. A is the projected area of the elastic contact. P_{\max} is the maximum indentation load and H is the hardness.

¹H NMR spectra

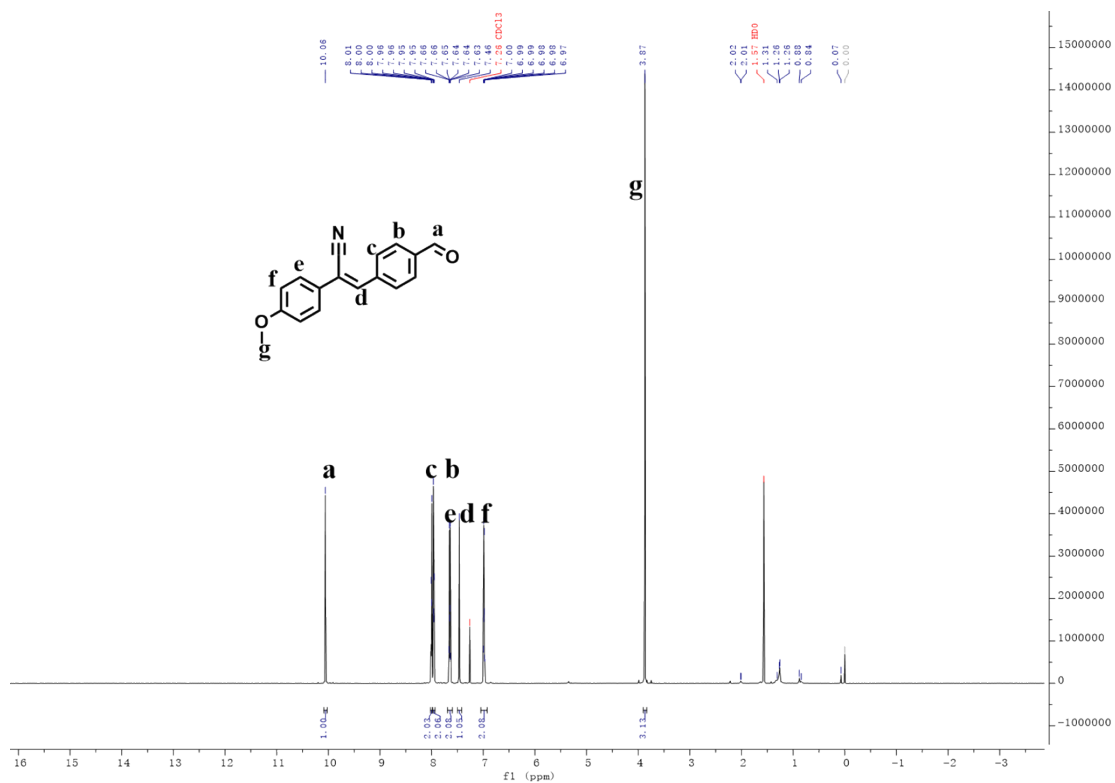


Fig. S1 ¹H NMR spectra of the (Z)-FMA (400 MHz, CDCl₃, 25°C, TMS). δ (ppm): 10.06(CHO, s, 1H), 8.00(Ar-H, $J = 8.0$ Hz, d, 2H), 7.96(Ar-H, $J = 8.0$ Hz, d, 2H), 7.65 (Ar-H, $J = 7.65$ Hz, m, 2H), 7.46 (-CH=CCN-, s, 1H), 6.98(Ar-H, $J = 6.99$ Hz, m, 2H), 3.87(OCH₃, s, 3H).

¹³C NMR spectra

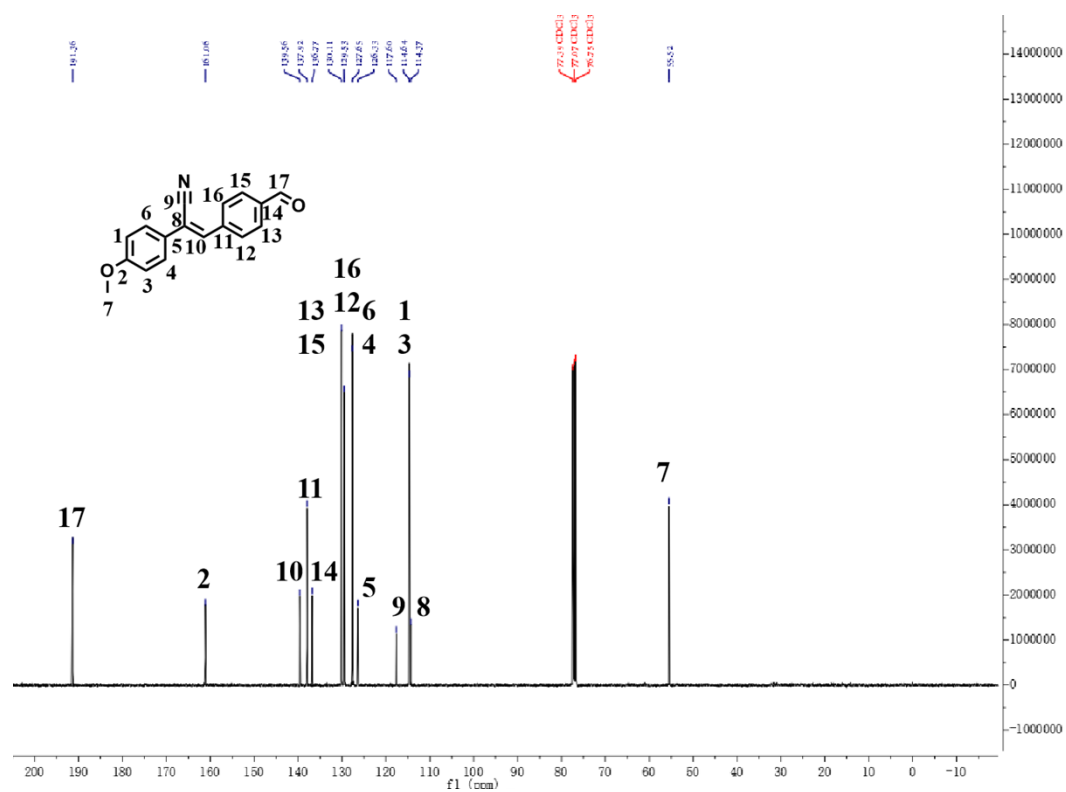


Fig. S2 ¹³C NMR spectra of the (Z)-FMA (400 MHz, CDCl₃, 25°C). δ (ppm): 191.32, 161.06, 139.56, 137.92, 136.77, 130.11, 129.53, 127.65, 126.33, 117.60, 114.64, 114.37, 55.52.

PXRD patterns of three polymorphs

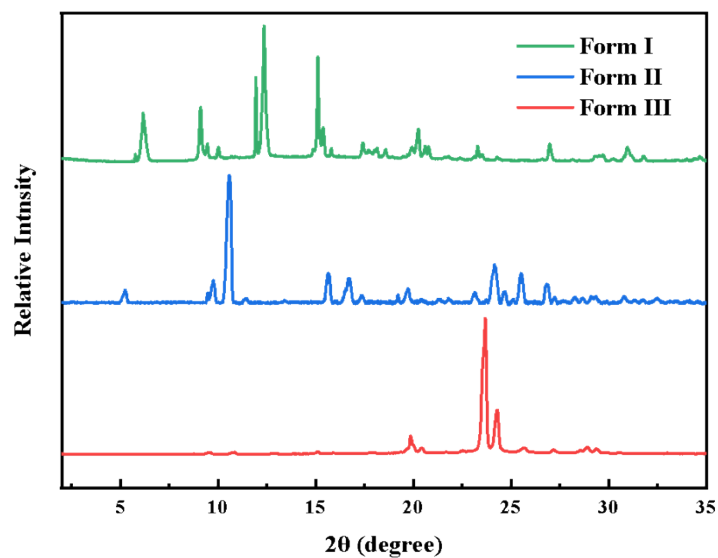


Fig. S3 PXRD patterns of Form I, Form II and Form III.

Face index

Face indexing of Form I was performed on the single crystal diffractometer (Bruker AXS Inc., D8 Venture, Germany). The major and minor side crystal faces were confirmed to coincide with the crystallographic (010) plane and (001) plane, which are perpendicular to the crystallographic b axis and c axis, respectively. The length direction of the crystal corresponds to the crystallographic a axis, constituting crystallographic (100) plane.

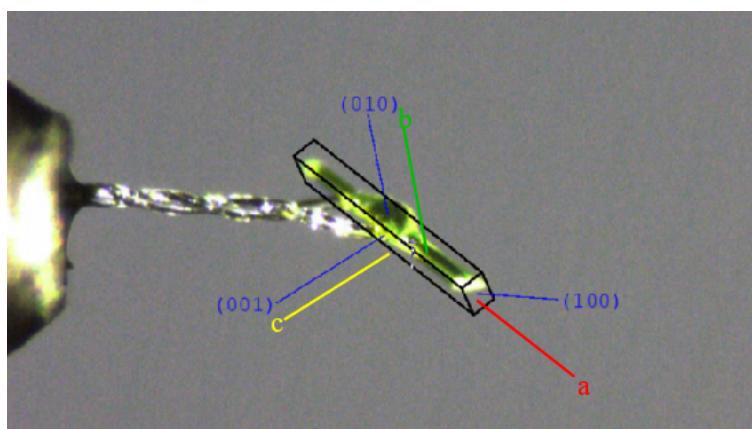


Fig. S4 Face index of Form I.

Stimulated face index

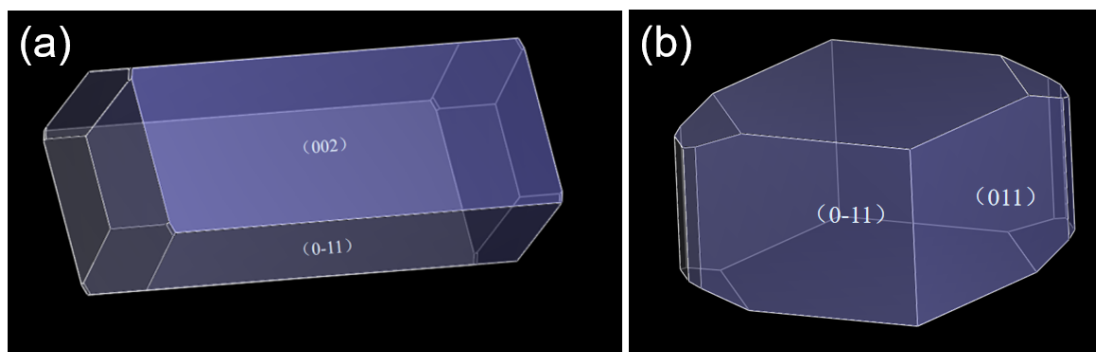


Fig. S5 Stimulated face index of Form II (a) and Form III (b).

Mechanical flexibility

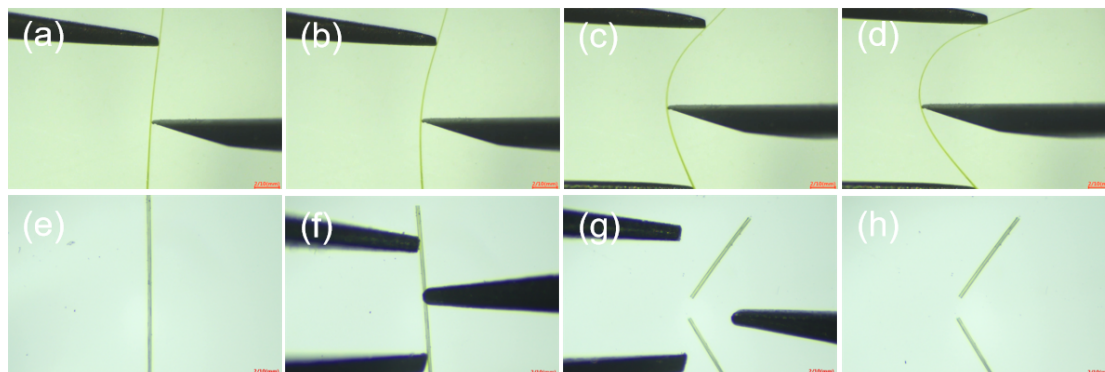


Fig. S6 (a-d) The mechanical flexibility of Form I. (e-f) The macroscopic brittleness of Form II.

Molecular stacking structure

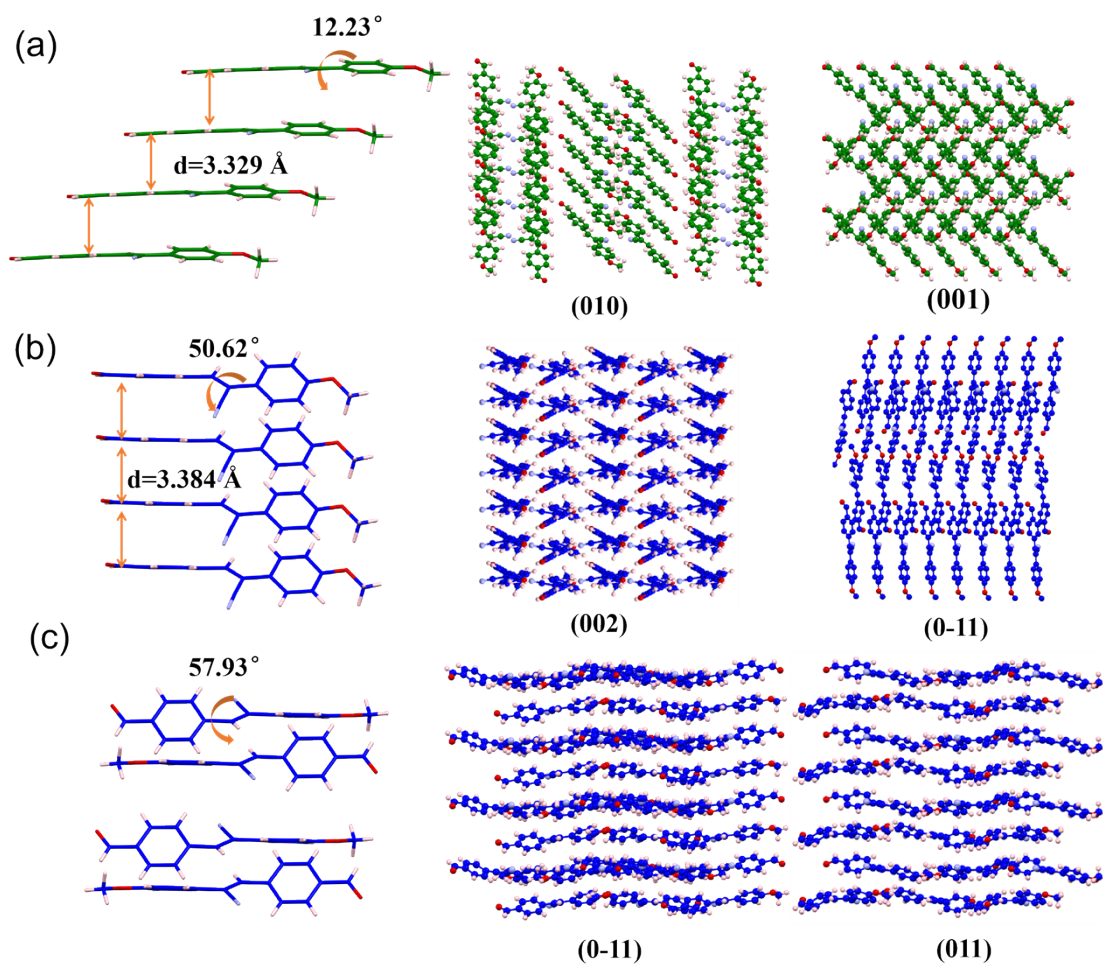


Fig.S7 The molecular conformations, π stacking mode of molecular columns and molecular stacking structure in Form I (a), Form II (b) and Form III (c) viewed from side planes.

Dipole moment

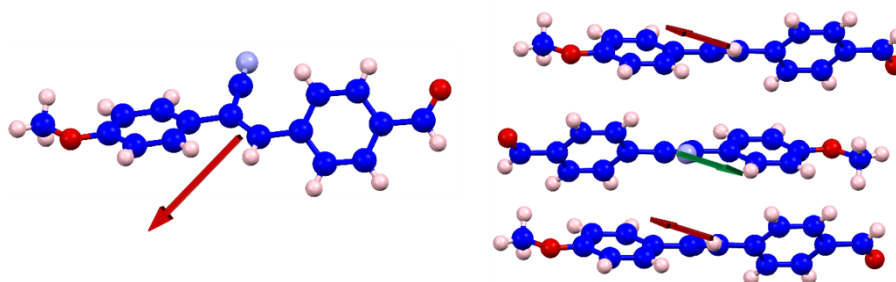


Fig. S8 The dipole moment direction of molecule in Form III.

Raman spectra

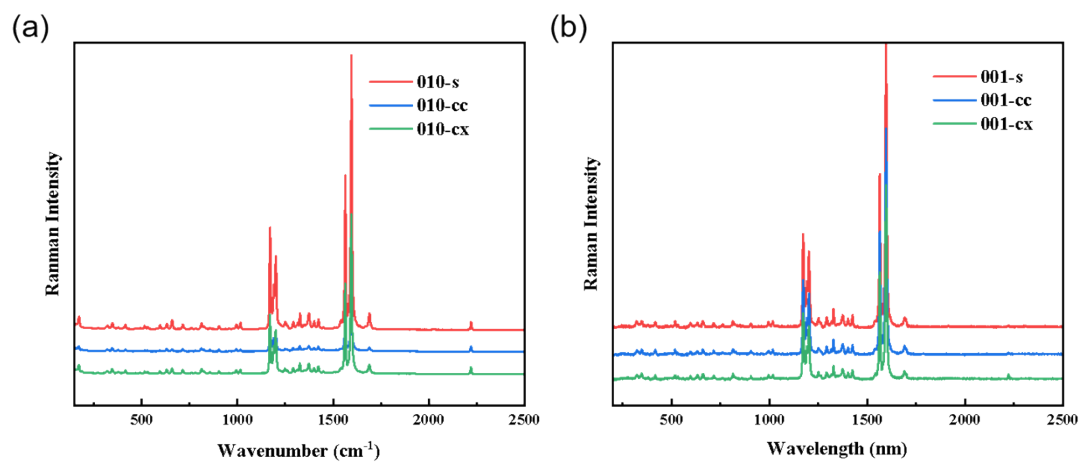


Fig. S9 Micro-Raman spectra were recorded for straight (s), concave(cc), convex(cx) regions of the (010) plane (a) and (001) plane (b).

Mechanical flexibility in liquid nitrogen

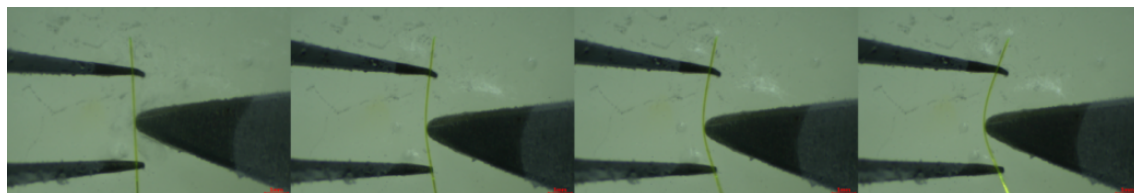


Fig. S10 Elastic bending process of Form I in liquid nitrogen (77K).

Crystal-to-crystal transition

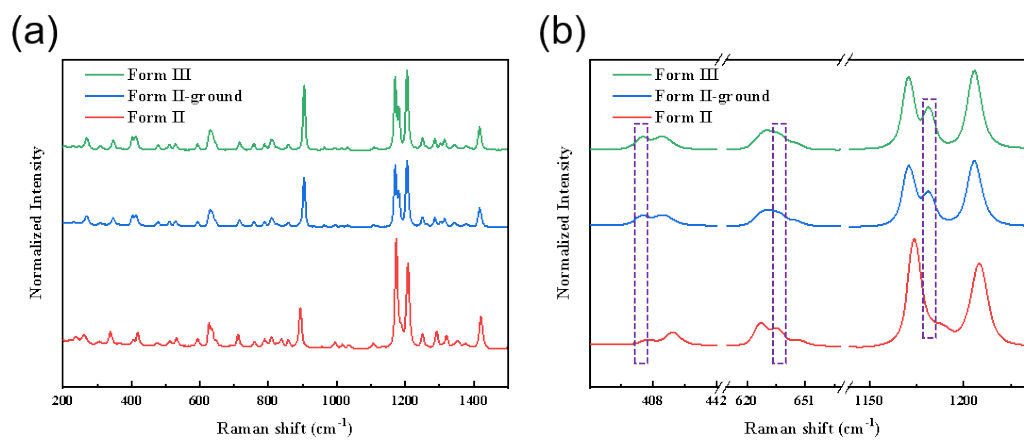


Fig. S11 Raman spectra were recorded for Form II, Form II-ground and Form III.

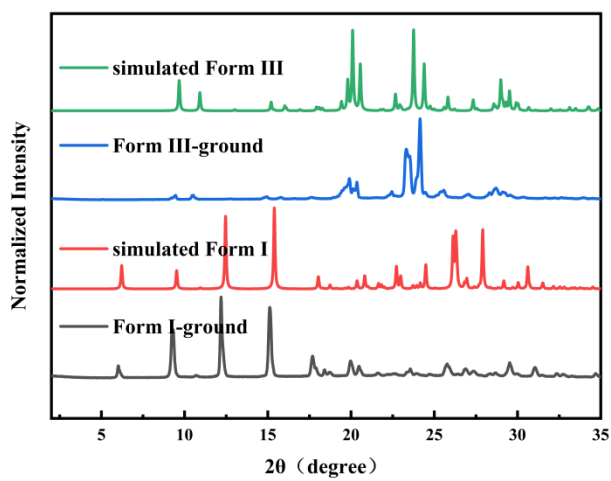


Fig. S12 The PXRD patterns of simulated Form I and Form III, ground Form I and Form III.

Thermal-induced crystal transition

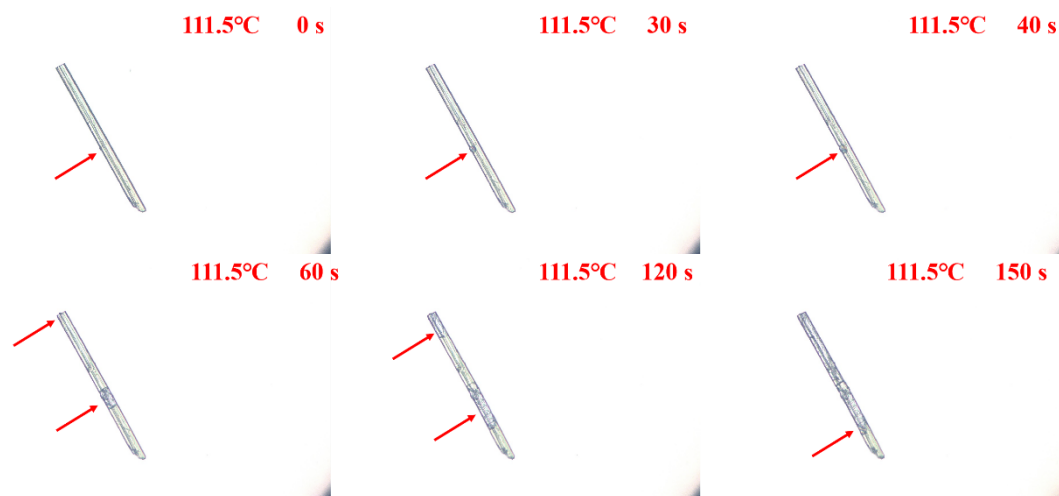


Fig. S13 The thermal induced phase transition of Form II in 111.5°C observed by polarizing light microscopy.

DSC curves

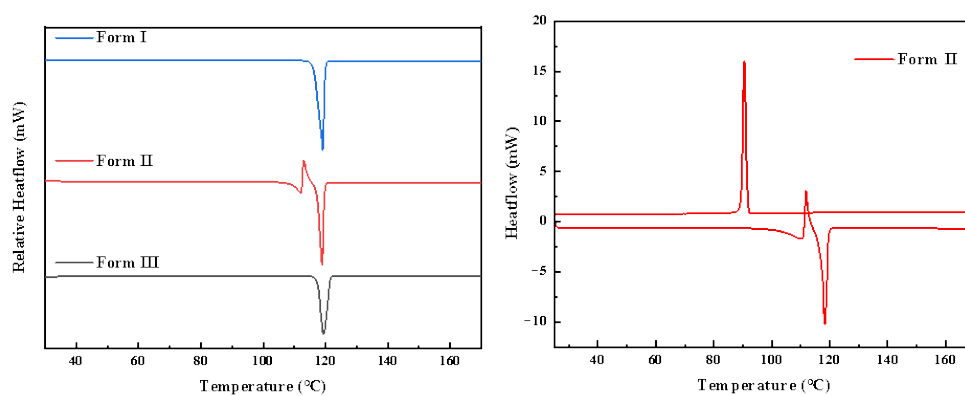


Fig. S14 (a) DSC curves of Form I to Form III. (b) Heating-cooling cycle in the DSC thermogram of Form II.

Fluorescence emission decay spectra

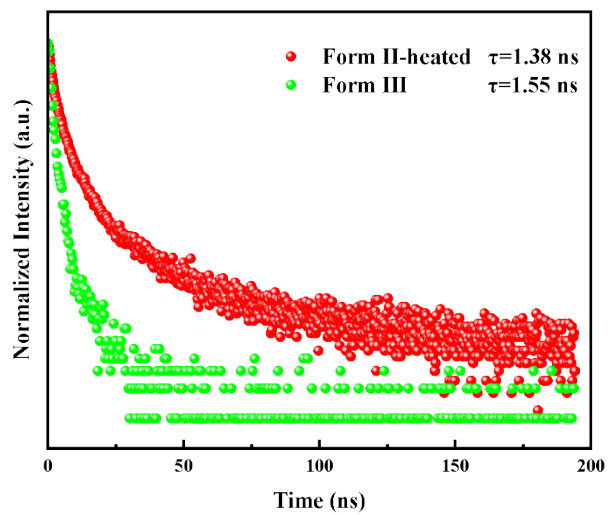


Fig. S15 Fluorescence emission decay spectra of heated Form II and Form III.

Energy Frameworks

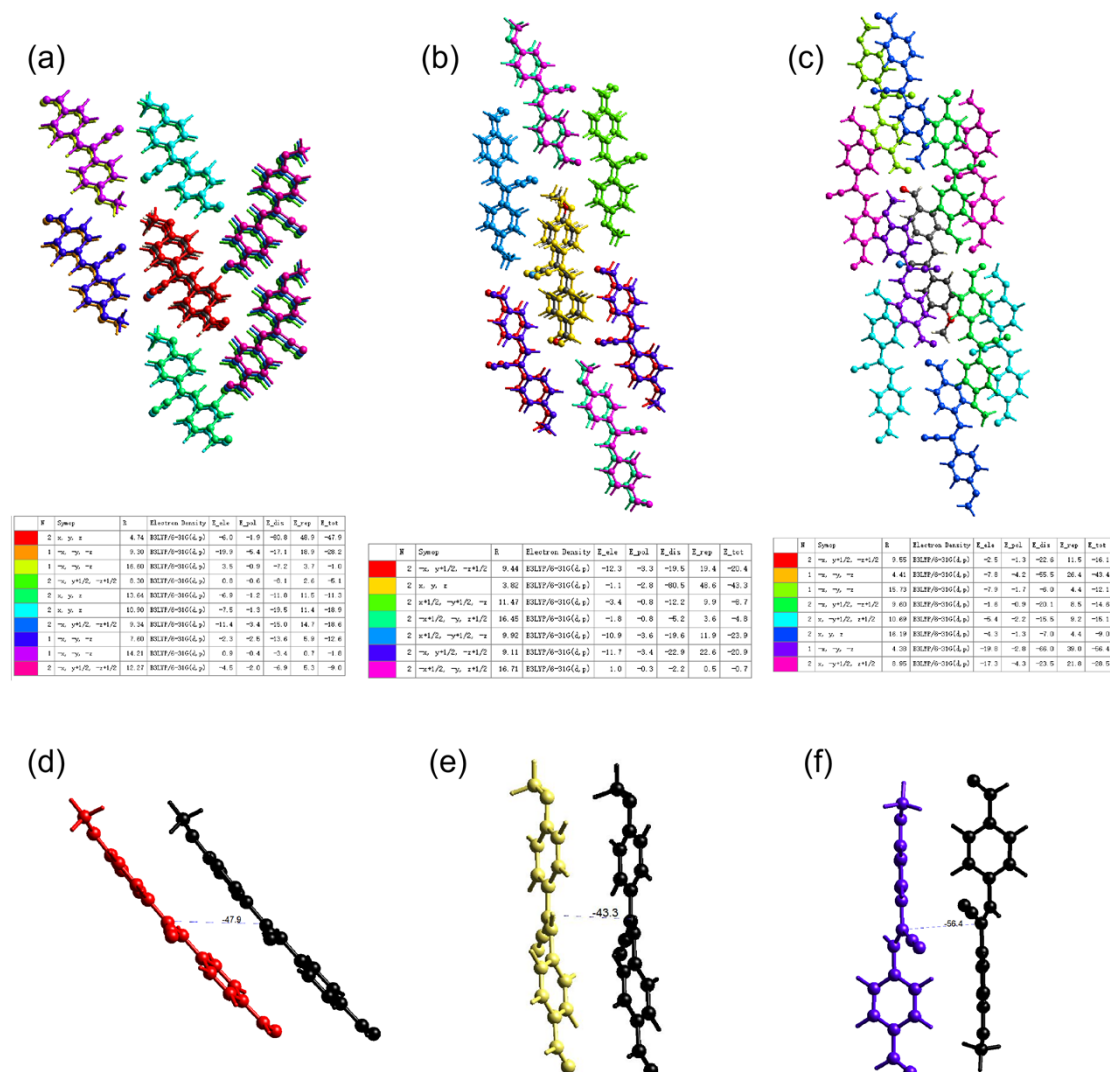


Fig. S16 Illustration of molecular interaction energies within 3.8 Å obtained from energy frameworks in Form I (a), Form II (b) and Form III (c). Illustration of calculated total interaction energies of π stacking in Form I (d), Form II (e) and Form III (f).

[2+2] cycloaddition

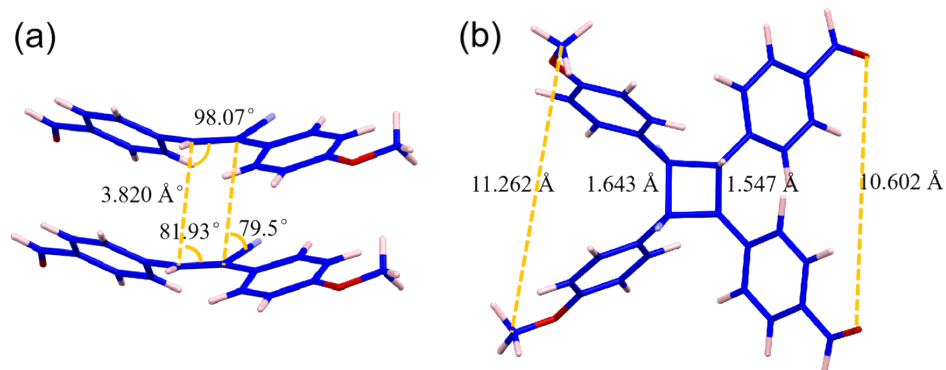


Fig. S17 (a) The distance between parallel vinyl double bonds of adjacent molecules in Form II. (b) The theoretical configuration of ' σ -dimer ([2 + 2] cycloadducts)' and corresponding distance.

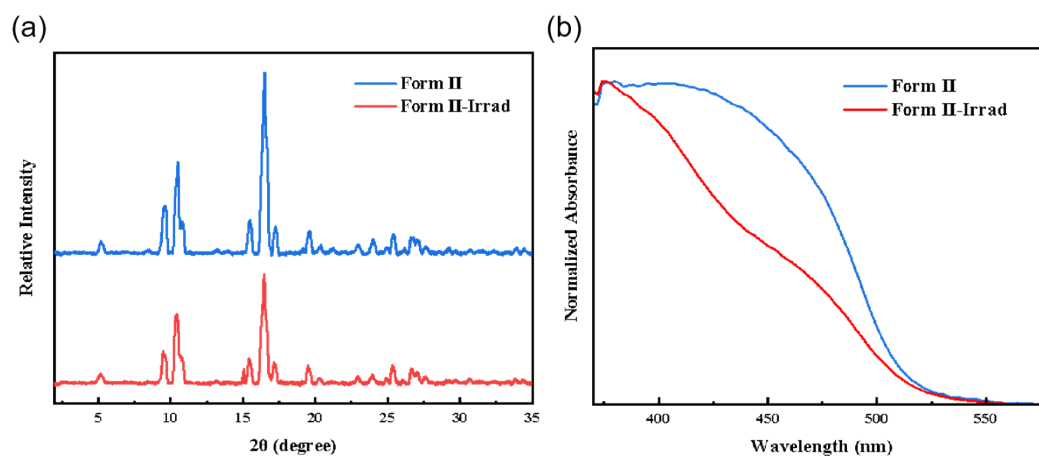


Fig. S18 PXRD patterns (a) and UV-vis absorbance spectra (b) of Form II before and after UV irradiation.

Crystallographic information

Table S1 Crystallographic information

	Form I	Form II	Form III
Formula	C ₁₇ H ₁₃ NO ₂	C ₁₇ H ₁₃ NO ₂	C ₁₇ H ₁₃ NO ₂
Formula weight	263.30	263.30	263.30
Crystal system	monoclinic	orthorhombic	monoclinic
Space Group	P21/c	P2 ₁ 2 ₁ 2 ₁	P21/c
a (Å)	4.7360(5)	3.8204(3)	7.4851(15)
b (Å)	9.8182(10)	10.5317(8)	16.192(3)
c (Å)	28.395(2)	32.715(3)	11.059(2)
α (°)	90	90	90
β (°)	90.950(9)	90	90.87(3)
γ (°)	90	90	90
V (Å ³)	1320.2(2)	1316.30(19)	1340.2(4)
Z	4	4	4
R ₁	6.43	5.38	5.57
WR ₂	17.32	11.22	15.96
CCDC number	2233988	2233987	2233986

Photophysical parameters

Table S2 The photophysical parameters of Form I to Form III.

	λ_{ex}	λ_{em}	$\Phi_F(\%)$	$\tau(\text{ns})$	$K_r(\times 10^7)$	$K_{\text{nr}}(\times 10^7)$
Form I	280	530	89.66	35.5	2.60	0.3
Form II	290	544	51.65	13.37	3.86	3.62
Form III	280	470	24.21	1.55	15.55	48.96

Reference

- 1 W. C. Oliver and G. M. Pharr, *Journal of Materials Research*, 2004, **19**, 3-20.